Changes in Electronic Structure and Chemical Bonding upon Crystallization of the Phase Change Material $GeSb_2Te_4$

A. Klein,[1] H. Dieker,[2] B. Späth,[1] P. Fons,[3] A. Kolobov,[3] C. Steimer,[2] and M. Wuttig[2]

[1]*Darmstadt University of Technology, Institute of Materials Science, D-64287 Darmstadt, Germany*

[2]*RWTH Aachen, I. Institute of Physics (IA), D-52056 Aachen, Germany*

[3]*Center for Applied Near-Field Optics Research (CAN-FOR), AIST, Tsukuba 305-8562, Japan*

(Received 6 January 2007; published 10 January 2008)

High-resolution photoelectron spectroscopy of *in situ* prepared films of $GeSb_2Te_4$ reveals significant differences in electronic and chemical structure between the amorphous and the crystalline phase. Evidence for two different chemical environments of Ge and Sb in the amorphous structure is found. This observation can explain the pronounced property contrast between both phases and provides new insight into the formation of the amorphous state.

DOI: 10.1103/PhysRevLett.100.016402 PACS numbers: 71.23.−k, 61.66.−f, 79.60.Ht, 82.80.Pv

Many Te and Sb alloys possess a remarkable property combination. They show a pronounced difference in optical and electronic properties between the amorphous and crystalline states, which makes them interesting for storage applications [1,2]. Such a finding can be accounted for only if the structural arrangement in the amorphous and crystalline states is sufficiently different. At the same time, this implies that significant atomic rearrangements are a prerequisite for crystallization of the amorphous phase. Hence, it seems surprising at first sight that crystallization in phase change materials can proceed on a nanosecond time scale. These findings are indicative of a unique correlation of atomic arrangement, physical properties, and transformation kinetics [3]. Indeed, it has recently been proven that in prototype phase change materials such as $Ge_2Sb_2Te_5$ and $GeSb_2Te_4$ the local atomic arrangement of the crystalline and amorphous states differs considerably [4,5]. This finding may provide an explanation for the changes in electronic structure that are crucial for applications of phase change materials in rewritable optical data storage and nonvolatile electronic memories. However, to derive an atomistic understanding of phase change materials, the detailed knowledge of the electronic structure and chemical bonding of these materials is a prerequisite. This knowledge is not only crucial for technological advances but also mandatory to achieve a fundamental understanding of these materials. Up to now, no direct experimental evidence for a pronounced change of electronic properties upon crystallization has been observed for phase change materials.

In this study the electronic structure and chemical bonding of $GeSb_2Te_4$ has been investigated by x-ray and ultraviolet photoelectron spectroscopy (XPS, UPS). $GeSb_2Te_4$ was chosen, since detailed *ab initio* calculations are available that describe the bonding in the amorphous and the metastable crystalline states [5]. Both states are prepared *in situ*. Thin films of $GeSb_2Te_4$ were deposited using dc magnetron sputtering. The sputtering chamber and the photoelectron spectrometer (ESCALAB 250) are part of the Darmstadt integrated system for solar cell research, which combines both chambers with an ultrahigh vacuum sample transfer [6]. The system allows for preparation and analysis of contamination-free films and surfaces. X-ray photoelectron spectra were recorded using monochromatic Al $K\alpha$ radiation with an analyzer pass energy of 10 eV, giving an overall experimental resolution of ~250 meV. The $GeSb_2Te_4$ films deposited at room temperature are amorphous as verified by x-ray diffraction. In order to crystallize the material, the sample was annealed at ~175 °C for 1 h in vacuum. The annealed sample shows the x-ray diffraction pattern of the rocksalt structure typical for the crystalline phase [7]. The XPS spectra of both samples show only Ge, Sb, and Te emissions.

Valence band spectra recorded using He I radiation are shown in Fig. 1. The onset of the valence band emission is considerably steeper after annealing (crystalline state), resulting in a strong increase of intensity between 0–1 eV binding energy. This difference corresponds well with electronic structure calculations involving a spinel-like local environment for the amorphous phase and a distorted rocksalt structure for the metastable crystalline state [5]. It can be related to the higher absorption coefficient of the crystalline state [8].

The Fermi energy of the amorphous state is expected to lie close to the middle of the energy gap as the activation energy for electronic transport is roughly half the size of the gap [9]. This is in very good agreement with our determined valence band maximum binding energy of 0.35 eV and an energy gap of 0.7 eV [10]. The valence band maximum of the crystalline phase lies closer to the Fermi energy. A shift of the valence band maximum towards the Fermi energy, which corresponds to an increased hole concentration, has been related to the formation of vacancies in the Ge and Sb sublattice [11,12]. Together with the improved structural order leading to a higher carrier mobility, the larger hole concentration is respon-

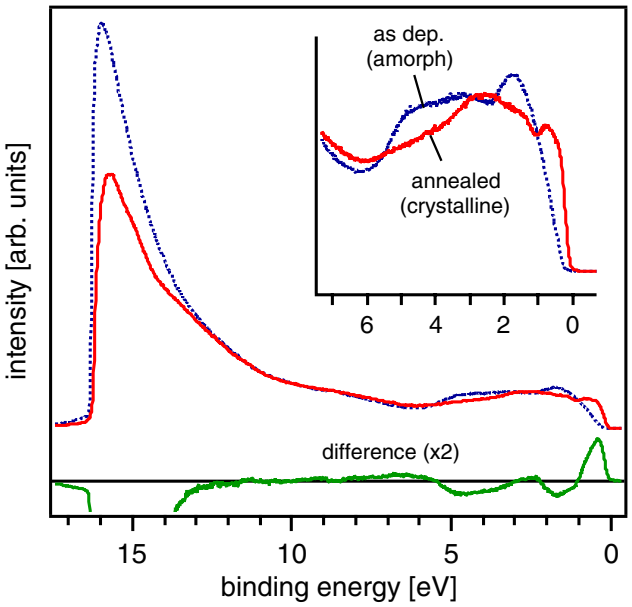

FIG. 1 (color online). Helium I excited valence band spectra of $GeSb_2Te_4$ deposited at room temperature (dotted blue line) and after annealing in vacuum (full red line).

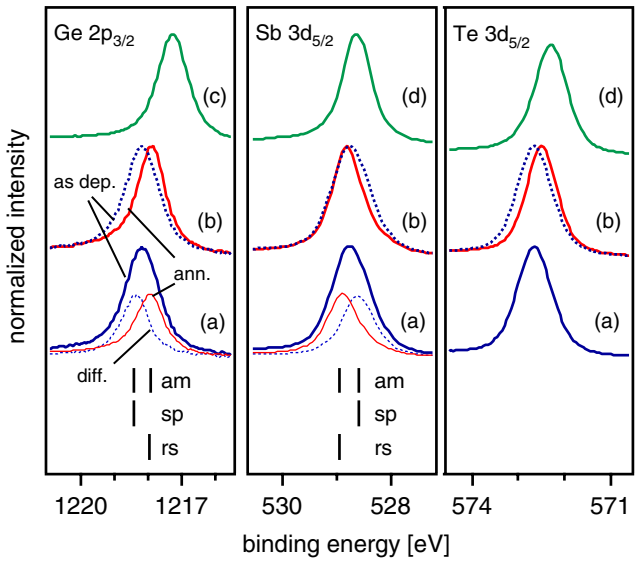

FIG. 2 (color online). Deep core-level spectra of $GeSb_2Te_4$ deposited at room temperature [full blue lines in (a) and dotted blue line in (b)] and after annealing [solid red line in (b)]. At the top, reference spectra from an amorphous Ge film (c) and from a crystalline Sb_2Te_3 film (d) are included. The Ge and Sb spectra of the as-deposited amorphous (am) $GeSb_2Te_4$ film can be deconvoluted into two components, which are identified with local environments corresponding to the rocksalt (rs) and spinel (sp) structures that are described in Ref. [5].

sible for the larger electrical conductivity of crystalline $GeSb_2Te_4$ compared to the amorphous state [9]. The upward shift of the valence band maximum after annealing amounts to 0.15–0.2 eV, which is very close to the reported decrease of the band gap [10].

While the differences in the valence band spectra help in understanding the optical contrast exploited in rewritable optical data storage, they do not provide information on the structural rearrangements underlying the changes in electronic structure. Differences in chemical bonding are, however, reflected in XPS, which will provide evidence for the presence of two different chemical environments of Ge and Sb in the amorphous state. For comparison, spectra were also recorded from crystalline Sb_2Te_3 and amorphous Ge.

For the identification of chemical changes using photoemission binding energies, it is often required to record data for photo- and Auger emissions. Because of the different charge of the photoemission (+1) and Auger (+2) final states, it is possible to distinguish between initial (chemical) and final state contributions to the binding energy shifts [13]. The latter are due to the screening of the core hole by polarization of the atom and lattice and therefore depend on the valence charge density and distribution. A 3 times larger shift of the Auger level as compared to that of the corresponding core level is expected if the changes in binding energy are only due to final state effects [13]. Such a behavior is observed here for the Te 3*d* core level (see Fig. 2), which exhibits a small shift (150 meV) towards lower binding energies after annealing. The shift of the Te MNN Auger line (not shown) is in the same direction and amounts to 450 meV, 3 times the shift of the core level. The changes of the Te binding energies upon the phase transition are therefore evidently related to a change in final state relaxation, which is associated with a change in free carrier concentration (see, e.g., Ref. [14]). As the carrier density is larger in the crystalline phase, an increased screening and hence lower binding energies are expected after annealing, in agreement with experiment.

In contrast to the Te emissions, the shift of the Ge LMM Auger line (700 meV) is less than 3 times the shift of the maximum of the Ge 2*p* level (300 meV). The Sb MNN line exhibits a shift of 280 meV to lower binding energies, which is in the opposite direction to the shift of the maximum of the Sb 3*d* core level (−50 meV). This analysis shows that the changes in the Ge and Sb core levels are partially due to initial state shifts, which are related to changes in chemical bonding.

Only small changes of line shape are observed upon crystallization for the Te 3*d* level where the full width at half maximum (FWHM) is slightly reduced as typical for a transition from an amorphous to a crystalline state. An identical effect is observed for the Te 4*d* level, which is shown together with the other shallow core levels in Fig. 3. The FWHM of the annealed sample agrees well with the FWHM of the crystalline Sb_2Te_3 sample. Overall, there are only small changes in the Te core levels supporting the conclusion that the changes in the Te emissions are mostly due to final state effects and only minor changes in the bonding state of Te between amorphous and crystalline $GeSb_2Te_4$ occur.

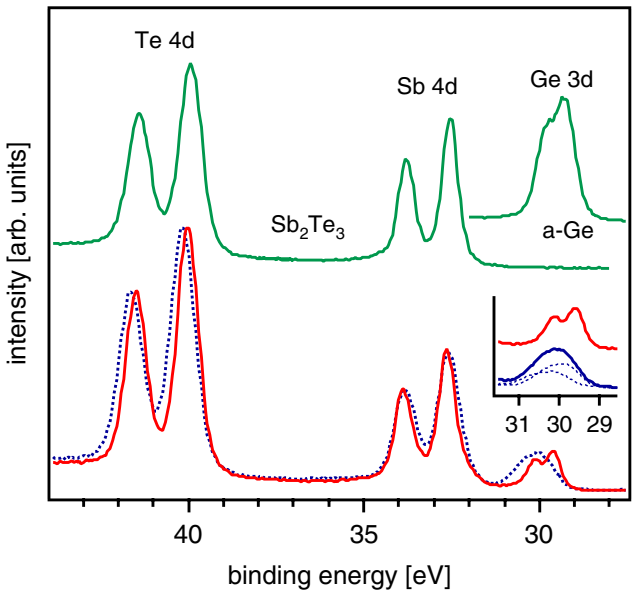

FIG. 3 (color online). Shallow core-level spectra of $GeSb_2Te_4$ deposited at room temperature (dotted blue line) and after annealing at 175 °C for 1 h (full red line). Reference spectra from a crystalline Sb_2Te_3 and an amorphous Ge film are also shown (full green line).

As evident from the comparison of the spectra shown in Fig. 2(b), the Ge $2p$ and Sb $3d$ levels of annealed $GeSb_2Te_4$ are considerably narrower than for the as-deposited film. However, the changes upon annealing cannot be explained by a simple narrowing of the peaks as expected for a transition between a disordered amorphous structure and an ordered crystalline structure that maintains the short range order. In contrast, the Ge $2p$ (Sb $3d$) level develops an asymmetry on the high (low) binding energy side, respectively. This means that the Ge $2p$ spectrum of the annealed film has a reduced intensity on the high binding energy side compared to the as-deposited film, while the Sb $3d$ spectrum has a reduced intensity on the low binding energy side. The asymmetric changes with annealing can be explained only if Sb and Ge are present in more than one chemical environment in the as-deposited (amorphous) film, which is not evident from the line shapes before annealing. It is further remarkable that the FWHM of the Ge $2p$ core level is broader for Ge in amorphous $GeSb_2Te_4$ than it is in amorphous Ge [Fig. 2(c)].

Because of the almost symmetric line shape of the Ge $2p$ and Sb $3d$ levels of the as-deposited film, curve fitting of the spectra using two components will not produce a unique result. We have therefore used difference spectra to test the hypothesis of two distinct chemical Ge and Sb environments. These were performed by multiplying the spectra of the crystalline film with an intensity factor and shifting them in energy. The resulting spectra were subtracted from the spectra of the as-deposited film. The intensity factor and energy shift were adjusted in order to obtain a symmetric line shape of the second components. In both cases the intensity factor is ~0.5 and the energy shift with respect to the crystalline state is less than 0.1 eV. The result of the deconvolution of the Sb $3d$ and the Ge $2p$ emission of the as-deposited film is depicted in Fig. 2(a). According to the deconvolution, the Sb $3d$ and Ge $2p$ spectra of the amorphous sample can be explained by two different components with binding energies of 528.9 and 528.6 eV for Sb $3d$ and 1217.95 and 1218.35 eV for Ge $2p$, respectively. The low (high) binding energy component of the Ge $2p$ (Sb $3d$) levels is identical to the component observed for the crystalline state and consequently associated with the chemical environment given by the rocksalt structure. The second component is shifted to higher (lower) energies for Ge (Sb), respectively.

Further evidence for the presence of two different chemical components in the amorphous structure is provided by the Ge $3d$ level, which is shown together with the other shallow core levels in Fig. 3. The peak recorded for the annealed sample can be fitted using a doublet with spin-orbit splitting of 0.56 eV and intensity ratio of 0.7 in agreement with literature [15]. A clear doublet structure is also observed for the amorphous Ge sample. In contrast, the as-deposited $GeSb_2Te_4$ film shows a very broad Ge $3d$ emission, which does not reveal the typical doublet structure. This emission can be fitted using two spin-orbit doublets with the same intensity ratio and spin-orbit splitting obtained for the crystalline film. The spectral weight and the energy separation between the two Ge components (0.4 eV) are in excellent agreement with the values derived from the Ge $2p$ core level.

The surface composition of the as-deposited and the annealed film differ by less than 10%, as particularly evident from the shallow core levels (Fig. 3). Surface segregation can therefore be ruled out as the origin of the spectral changes.

The core-level photoemission spectra can be consistently described by assuming two different chemical environments of Ge and Sb in the amorphous state. The single chemical environment for the crystalline phase compares well with the distorted rocksalt structure, where all Ge and Sb positions are identical [5]. It has recently been suggested that a small fraction of Ge atoms form homopolar bonds (i.e., Ge-Ge bonds) [16]. Such a finding does not provide a straightforward explanation of the results obtained here as we observe a second environment for Ge *and* Sb atoms, and the deconvolution of the spectra implies that roughly half of the Ge and Sb atoms are in an atomic arrangement not found in crystalline $GeSb_2Te_4$. This raises the question of the atomic arrangement responsible for the second Ge and Sb peak. For the additional components of Ge (Sb) in the amorphous phase, according to their relative binding energies with respect to the crystalline phase, a higher (lower) partial oxidation is indicated. Assuming that Ge and Sb only form chemical bonds to Te, this should correspond to a reduced (increased) length of the Ge-Te

(Sb-Te) bonds, respectively. These are in accordance with the recently proposed spinel structure of the amorphous phase [5]. In this structure, the Ge atoms have a reduced distance to the Te atoms as compared to the distorted rocksalt structure, while the Sb atoms have an increased distance to the Te atoms. This changes the bond strength and the charge transfer between the neighbors. We therefore suggest that the amorphous phase of $GeSb_2Te_4$ consists of two local arrangements that locally resemble the distorted rocksalt structure and the spinel structure, respectively. Such a finding is not inconsistent with the density-functional theory calculations, which show that the energy difference between the spinel and the rocksalt structure is quite small. Hence, it is plausible that the amorphous state consists of both local environments.

Our data are further in excellent agreement with high-energy XPS measurements ($h\nu = 4345$ eV), which reduce the importance of surface effects. That surface effects do not contribute to the spectral changes is already indicated by the comparable changes upon crystallization in the shallow and deep core levels. In the high-energy experiments, 35 nm $GeSb_2Te_4$ layers were grown between $(ZnS)_{0.85}(SiO_2)_{0.15}$ cladding layers on silica substrates. A 100 nm Al-Cr alloy layer was deposited on the surface as a heat sink. A disk testing unit (Pulsetech DDU-1000) was then used to laser reamorphize and recrystallize regions via the substrate side of the sample. The reversibility of the process was confirmed employing the same tester, reproducing the expected increase of reflectance upon recrystallization and the decrease of reflectance upon reamorphization, respectively. The top Al and $(ZnS)_{0.85} \times (SiO_2)_{0.15}$ layers were removed immediately before photoelectron measurements using dilute HF solution. The spectrometer was attached to beam line bl15xu at SPring-8. Only very weak C 1*s* and O 1*s* peaks were detected in survey scans. The use of an electron flood gun was required for the laser reamorphized sample to overcome charging effects; the effects of the gun were accounted for in the analysis by use of the fortuitous C 1*s* peaks. The energy resolution of the incident x-ray beam was ~50 meV. The observed energy shifts of −32 meV (Sb 3*d*), 146 meV (Te 3*d*), 145 meV (Te 4*d*), and −25 meV (Sb 4*d*) were all within 20 meV of the values determined using the DAISY-SOL system strongly supporting the results reported above and at the same time directly linking the results to the laser recrystallized and laser reamorphized states of $GeSb_2Te_4$.

In summary, photoelectron spectroscopy of *in situ* prepared and annealed $GeSb_2Te_4$ phase change compound exhibits significant differences in electronic structure including a large increase in density of states in the upper valence band region and an upward shift of the valence band maximum. Core-level spectra indicate that Ge and Sb are present in two different environments in the amorphous phase. This implies that the amorphous state is a mixture of atoms arranged in a tetrahedral and an octahedral arrangement of Ge atoms. This finding is consistent with the observed optical properties, i.e., can explain the pronounced change in optical properties upon the crystallization of amorphous $GeSb_2Te_4$ [8] and should also be able to explain the change of structural order observed by extended x-ray-absorption fine structure spectroscopy. The most interesting question to address is how a coexistence of different sites is created in the amorphous structure of $GeSb_2Te_4$. This question calls for a detailed study of the structure of the liquid state and motivates theoretical studies employing novel concepts such as speciation to describe the structure of the amorphous state [17].

Financial support by the Deutsche Forschungsgemeinschaft (No. Wu 243/11) is gratefully acknowledged. High-energy XPS was carried out at SPring-8 approved by JASRI under the Nanotechnology Support Project of the MEXT (No. 2005A0564-CSa-np-Na/ BL-No.15XU).

[1] S. Ovshinsky, Phys. Rev. Lett. **21**, 1450 (1968).
[2] N. Yamada, MRS Bull. **21**, 48 (1996).
[3] A. L. Greer and N. Mathur, Nature (London) **437**, 1246 (2005).
[4] A. V. Kolobov, P. Fons, A. I. Frenkel, A. L. Ankudinov, J. Tominaga, and T. Uruga, Nat. Mater. **3**, 703 (2004).
[5] W. Welnic, A. Pamungkas, R. Detemple, C. Steimer, S. Blügel, and M. Wuttig, Nat. Mater. **5**, 56 (2006).
[6] J. Fritsche, A. Klein, and W. Jaegermann, Adv. Eng. Mater. **7**, 914 (2005).
[7] T. Matsunaga and N. Yamada, Phys. Rev. B **69**, 104111 (2004).
[8] W. Welnic, S. Botti, L. Reining, and M. Wuttig, Phys. Rev. Lett. **98**, 236403 (2007).
[9] I. Friedrich, V. Weidenhof, W. Njoroge, P. Franz, and M. Wuttig, J. Appl. Phys. **87**, 4130 (2000).
[10] B.-S. Lee, J. R. Abelson, S. G. Bishop, D.-H. Kang, B.-K. Cheong, and K.-B. Kim, J. Appl. Phys. **97**, 093509 (2005).
[11] A. H. Edwards, A. C. Pineda, P. A. Schultz, M. G. Martin, A. P. Thompson, H. P. Hjalmarson, and C. J. Umrigar, Phys. Rev. B **73**, 045210 (2006).
[12] M. Wuttig, D. Lüsebrink, D. Wamwangi, W. Welnic, M. Gillessen, and R. Dronskowski, Nat. Mater. **6**, 122 (2007).
[13] W. F. Egelhoff, Jr., Surf. Sci. Rep. **6**, 253 (1987).
[14] Y. Gassenbauer, R. Schafranek, A. Klein, S. Zafeiratos, M. Hävecker, A. Knop-Gericke, and R. Schlögl, Phys. Rev. B **73**, 245312 (2006).
[15] R. D. Bringans, M. A. Olmstead, R. I. G. Uhrberg, and R. Z. Bachrach, Phys. Rev. B **36**, 9569 (1987).
[16] D. A. Baker, M. A. Paesler, G. Lucovsky, S. C. Agarwal, and P. C. Taylor, Phys. Rev. Lett. **96**, 255501 (2006).
[17] M. Micoulaut, Phys. Rev. B **74**, 184208 (2006).